Cellular Oncology 30 (2008) 27–38
IOS Press

Protein profiling of B-cell lymphomas using tissue biopsies: A potential tool for small samples in pathology

Corine Jansen [a,*], Konnie M. Hebeda [a], Marianne Linkels [a], Johanna M.M. Grefte [a], John M.M. Raemaekers [b], Johan H.J.M. van Krieken [a] and Patricia J.T.A. Groenen [a]

[a] *Dept. of Pathology, Radboud University Nijmegen Medical Centre, The Netherlands*
[b] *Dept. of Hematology, Radboud University Nijmegen Medical Centre, The Netherlands*

Abstract. Non-Hodgkin's lymphoma comprises many related but distinct diseases and diagnosis and classification is complex. Protein profiling of lymphoma biopsies may be of potential value for use in this lymphoma classification and the discovery of novel markers. In this study, we have optimized a method for SELDI-TOF MS based protein profiling of frozen tissue sections, without dissection of tumour cells. First we have compared chip surfaces and lysis buffers. Also, we have determined the minimal input using laser dissection microscopy. Subsequently, we have analyzed and compared protein profiles of diffuse large B-cell lymphoma ($n = 8$), follicular lymphoma ($n = 8$) and mantle cell lymphoma ($n = 8$). Benign, reactive lymph nodes ($n = 14$) were used as a reference group.

CM10 chip surface in combination with urea lysis buffer and an input of approximately 50,000 lymphocytes allowed the detection of many differential peaks. Identification of the diffuse large B-cell lymphoma cases was reliably made in the supervised classification. Unsupervised clustering showed segregation into a benign/indolent cluster predominantly formed by benign, reactive lymph nodes and follicular lymphoma cases and into a more aggressive cluster formed by diffuse large B-cell lymphoma and mantle cell lymphoma cases. In conclusion, our protocol enables protein profiling of protein lysates derived from small histological samples and the subsequent detection of many differentially expressed proteins, without the need of tumour cell dissection. These results support further evaluation of protein profiling of small lymphoma biopsies as an additional tool in pathology.

Keywords: Classification, non-Hodgkin's lymphoma, protein profiling, proteomics, SELDI-TOF MS

Abbreviations

B-NHL:	B-cell non-Hodgkin's lymphoma,
DLBCL:	diffuse large B-cell lymphoma,
FL:	follicular lymphoma,
LDM:	laser dissection microscopy,
MCL:	mantle cell lymphoma,
SELDI-TOF MS:	surface enhanced laser dissection/ionization time-of-flight mass spectrometry.

1. Introduction

Non-Hodgkin's lymphoma (NHL) diagnosis is based on classification according to the World Health Organization Classification [1] by integrating morphological, immunochemical and molecular features. Pathological diagnosis is primarily based on the use of tissue biopsies. For classification of the different B- and T-cell entities, immunohistochemistry using antibodies against marker proteins is an important supplementary technique. The continuous recognition of new clinical and biological disease entities requires a growing arsenal of techniques for classification and detection of new prognostic and therapeutic markers. The use of mass spectrometry based techniques for protein profiling of diagnostic tissue samples is expected to meet these requirements as it enables the simultaneous analysis of many different proteins.

Protein profiling techniques that require relatively low amounts of diagnostic input material are liquid chromatography-MS/MS, which has successfully been applied in human anaplastic large cell lymphoma [2,3] and in follicular lymphoma-derived cells

*Corresponding author: Corine Jansen, 824 Dept. of Pathology, Radboud University Nijmegen Medical Centre, P.O. Box 9101, 6500 HB Nijmegen, The Netherlands. Tel.: +31 24 361 89 45; Fax: + 31 24 366 8750; E-mail: c.jansen@pathol.umcn.nl.

[4], and ProteinChip™ technology. The last technology is based on an application of mass spectrometry called Surface Enhanced Laser Desorption/Ionization-Time of Flight Mass Spectrometry (SELDI-TOF MS) that enables simultaneous on-chip binding and high throughput analysis of small, complex diagnostic protein samples. SELDI-TOF MS based protein profiling has successfully been applied for the discrimination between normal and disease in serum samples [5–11], whole tissues [12], and laser dissected tissues [13,14]. SELDI-TOF MS also assisted in the discovery of potentially new biomarkers in different carcinomas [15–18].

In the present study we have optimized the SELDI-TOF MS application for diagnostic frozen tissue sections of different categories of malignant lymphoma. This was done by comparing two different chip types in combination with two different lyses buffers. To assess the clinical applicability of the method for small samples like i.e. core needle biopsies or cytological specimens, the minimal amount of input material required for SELDI-TOF MS was evaluated. In addition, we have evaluated this optimized SELDI-TOF MS method using complex protein samples prepared from undissected frozen histological specimens to see if this method actually enables detection of differential proteins that enable lymphoma classification. For this purpose, we focused on the discrimination of benign lymph nodes from three different malignant B-cell lymphoma types. A recent paper by Fan et al. [19] describes the successful differentiation by protein profiling of low grade follicular lymphoma (FL) from the rare but aggressive Burkitt lymphoma and reactive follicular hyperplasia. For clinical application, comparison of the more common lymphomas such as diffuse large B-cell lymphoma (DLBCL) that constitute 30–40% of all lymphoma's is relevant as well. Lin et al. studied matched pairs of FL and DLBCL counterparts from two patients and demonstrated the detection of differentially expressed proteins like cyclin D3 and caspase3 [20].

Our study includes three common lymphoma types that are characterized by a different phenotype, molecular background, clinical behaviour and outcome. FL represents a lymphoma with indolent clinical behaviour. DLBCL is the most common group of lymphoma with a histological intermediate behaviour, although clinically heterogeneous. Mantle cell lymphoma (MCL) is a more rare disease and has an adverse clinical course. The group of benign lymph nodes in our study includes reactive follicular hyperplasia, T-cell hyperplasia and sinus histiocytosis, thereby representing a large part of the spectrum of benign nodes that are seen in a routine diagnostic setting. We have analyzed protein lysates prepared from frozen tissue of archival, routinely diagnosed cases. Our study shows the potential value of protein profiling.

2. Materials and methods

2.1. Samples included in the classification study

Diagnostic frozen tissue samples were obtained from the archive of the Department of Pathology, Radboud University Nijmegen Medical Centre, Nijmegen, the Netherlands. Samples were obtained according to the Code Proper Secondary Use of Human Tissue [21]. All NHL samples were classified according to the World Health Organization Classification [1]. For this study we used lymph node biopsies containing DLBCL ($n = 8$), FL ($n = 8$) (FL cases 2 and 5 are of grade I and the six other FL cases are of grade III) and MCL ($n = 8$). Tumour load varied, ranging from 50–90%. Benign lymph nodes (RL, $n = 14$) were used as a reference group and these cases harboured different amounts of common hyperplasia types.

2.2. Chip information and sample preparation

In order to optimise the protocol for profiling of tissue lysates, the CM10 (cationic exchange) and the Q10 (anionic exchange) chip surfaces were compared together with two different lysis buffers: an UTC lysis buffer (6 M Urea, 2 M thio-urea, 2% (w/v) Chaps, 1% (w/v) DTT, Protease Inhibitor Cocktail (Roche Diagnostics, Mannheim, Germany)) and an Imidazole lysis buffer (10 mM, pH 7).

For sample preparation, approximately 200 mm^2 of 10 μm thick frozen tissue sections was obtained from each case. These sections were homogenized in 100 μl lysis buffer per 100 mm^2. Samples were drawn through an 0.8 mm needle, incubated for one hour at room temperature, and centrifuged (13,000g, 10 min at room temperature) to remove cell debris. Protein concentrations were quantified with the 2D-Quant Kit (Amersham Biosciences, San Francisco). All concentrations were adjusted to 400 ng/μl and 10 μl aliquots were stored at -80°C. Adjacent frozen tissue sections (4 μm) were Hematoxylin and Eosin stained to provide information on tumour load or, in case of the benign lymph nodes, on hyperplasia. Technical duplicates were randomized over the chips.

2.3. Chip loading

Protein samples were analyzed in duplicate on CM10 and Q10 ProteinChips™ (Ciphergen Biosystems, Fremont, California). A control sample was used to determine the %CV values. Before chip loading, 90 µl Acetate binding buffer (0.1 M ammonium acetate, pH 4.5, 0.1% Triton X-100) was added to each 10 µl sample aliquot (containing 4 µg protein) for the CM10 chips. For the Q10 chips, 90 µl of Tris binding buffer (0.1 M Tris-HCl, pH 8.0) was added to each sample. To remove counter ions, the chips were bulk washed briefly in 10 mM HCl. After placing the chips into the Bioprocessor (Ciphergen Biosystems), spots were washed twice with 200 µl binding buffer for 5 minutes at 600 RPM at room temperature, incubated at 600 RPM for 45 minutes at room temperature, washed twice with binding buffer to remove unbound proteins, and twice with chip type specific washing buffer (chip type specific binding buffer without Triton X-100) in order to remove traces of Triton X-100; all washing steps were performed during 5 minutes at 600 RPM at room temperature. After a brief wash with 5 mM HEPES, pH 7.0, chips were removed from the Bioprocessor and left to dry during 15 minutes. A saturated solution of the energy absorbing molecule sinapinic acid, prepared in 50% (v/v) acetonitrile and 0.5% (v/v) trifluoroacetic acid was applied to each spot twice (2×1 µl). In order to obtain good crystallization of the proteins bound to the chip, spots were left to dry for 5 minutes after each SPA application.

2.4. Generating mass spectra

The PBS IIc mass spectrometer (Ciphergen Biosystems), supplemented with an autoloader, was used to generate Time of Flight (TOF) mass spectra in the range 0–50,000 Da using Protein Chip Software (Ciphergen Biosystems). Spectra were obtained with the following instrument settings: laser energy low 170/high 190, deflector mode set at 1,000 Da, optimization range was set at 3,000–20,000 Da (focus by optimization centre). Measurements within a spot were performed from position 20–80, with delta 2, collecting 50 transients per position, and hard shots (at laser energy 190) were excluded from the averaged data. Protein Standard (Ciphergen Biosystems) was used for external calibration and measured at identical instrument settings as the samples. All spectra were preprocessed using Protein Chip Software. The spectra were base-line subtracted and noise detection was set from 2,000 Da up to 50,000 Da without smoothing and with a fitting width of eight times the expected peak width.

2.5. Minimal input determination and hyperplasia comparison using laser dissection microscopy

SELDI-TOF MS has successfully been applied for protein profiling of small numbers of epithelial cells in the context of carcinoma. As B-lymphocytes contain less cytoplasm than epithelial cells, we have determined the minimal input of lymphoid tissue. The minimal number of cells necessary for profiling was assessed by analyzing lysates prepared from different numbers of germinal centre B-cells. Independent samples, containing approximately 48,000, 24,000, 12,000, 6,000, 3,000, and 1,500 germinal centre cells were collected from hematoxylin stained benign lymph node sections with follicular hyperplasia using laser dissection with a Leica AS LDM microdissection system with a UV laser (Leica Microsystems Wetzlar GmbH, Germany). The dissected cells were subsequently homogenized in 12 µl UTC lysis buffer and stored at -80°C. The protein concentration of a protein lysate of approximately 50,000 cells was quantified with the 2D-Quant Kit. All samples were loaded on CM10 chips and analyzed as described above.

For a few additional reactive lymph node cases, different hyperplastic areas were dissected and used for comparison of their protein profiles. These hyperplasia types were follicular hyperplasia that mainly consists of B-cells, paracortical hyperplasia which predominantly contains T-cells, and sinus histiocytosis that shows an increase of fibrosis, sinus expansion and sinus histiocytes. For each hyperplasia type, comparable areas (corresponding to approximately 50,000 B-cells) were obtained with laser micro dissection from hematoxylin stained frozen tissue sections and processed as described above.

2.6. Data analysis

Samples were analyzed on different days. In order to correct for inter-experiment variation, spectra with comparable averaged total ion currents (AveTIC) and protein profiles were included in the analysis. Selected spectra were exported to CiphergenExpress™, mass aligned and normalization was performed from 2,000 Da up to 50,000 Da using an external normalization coefficient of 0.2. Cluster detection was performed with signal-to-noise threshold for the first pass

peak detection at 8.0, and peaks should be present in at least 12% of all spectra. For the second pass peak detection, a signal-to-noise threshold at 2.0 was used and estimated peaks were included. Generated peak clusters were analyzed (CiphergenExpress^{TM}) to detect differentially expressed protein peaks. In addition to this supervised approach, data were analyzed using unsupervised hierarchical clustering.

3. Results

3.1. Optimizing SELDI-TOF MS application for lymphoma tissue samples

To select a method that would give sufficient peaks to enable protein profiling, we have tested two different lysis buffers and different chip surfaces, a cationic (CM10) and an anionic (Q10) chip surface. Spectra generated on the Q10 chips showed relatively few peaks for both buffers in the range of 6,000–16,000 M/Z (Fig. 1C and D: 9,000–16,000 M/Z). The combination of CM10 chip and Urea/UTC buffer (Fig. 1A) resulted in detection of the highest number of peaks; 94 unique peaks with a signal/noise $\geqslant$2. Because the presence of many peaks makes detection of differential protein present in the different lymphoma subtypes more likely, the last combination was used for further experiments.

In order to determine the minimal input for profiling, protein lysates were generated from different numbers of laser dissected germinal centre cells that were stained with Hematoxylin. The Hematoxylin staining of the sections prior to dissection did not interfere with the SELDI-TOF MS procedure (data not shown). Highly similar mass spectra were obtained

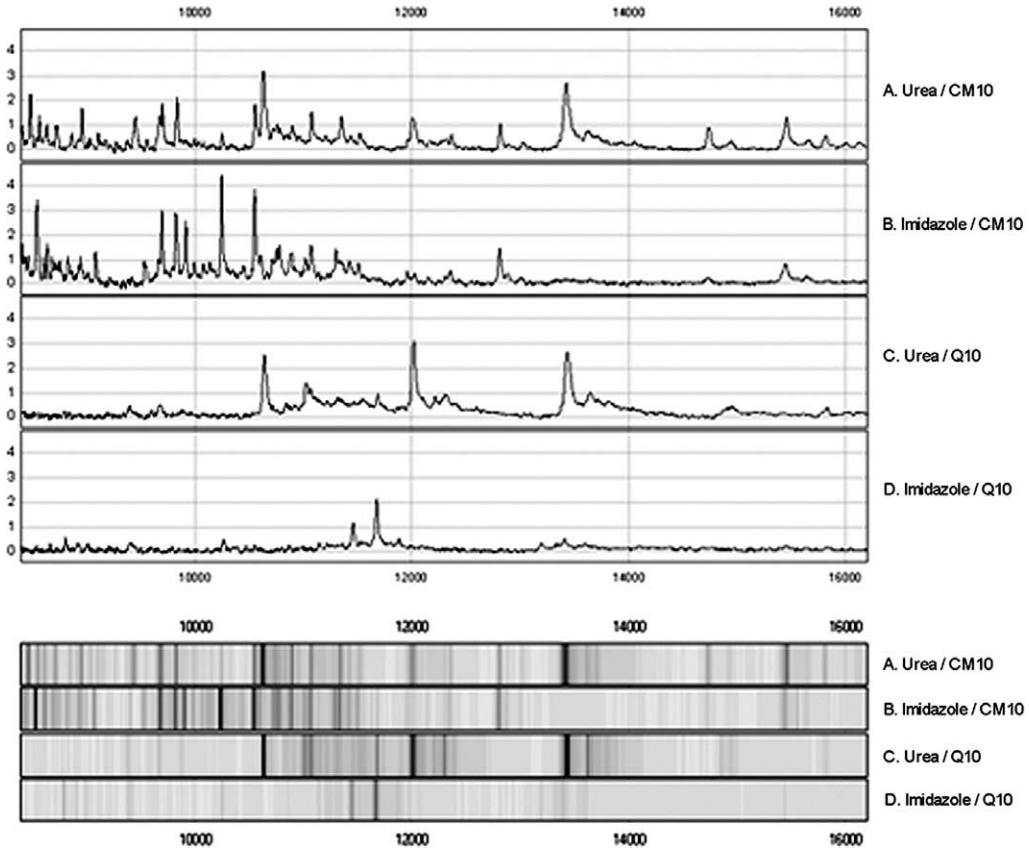

Fig. 1. Comparison of different chip surfaces and lysis buffers for the generation of protein profiles from frozen tissue sections. Frozen tissue sections from a benign reactive lymph node were homogenized in Urea lysis buffer and Imidazole lysis buffer. Equal amounts of protein were loaded onto CM10 and Q10 chips. The upper panel shows a segment of the resulting mass spectra in the range of 9,000–16,000 M/Z (X-axis). The relative peak intensities are plotted along the Y-axis. The combination of the Urea lysis buffer and CM10 chip surface allows detection of more proteins as compared to the other combinations tested. In the lower panel, the spectra from the upper panel are visualized as gel traces (*gel view*).

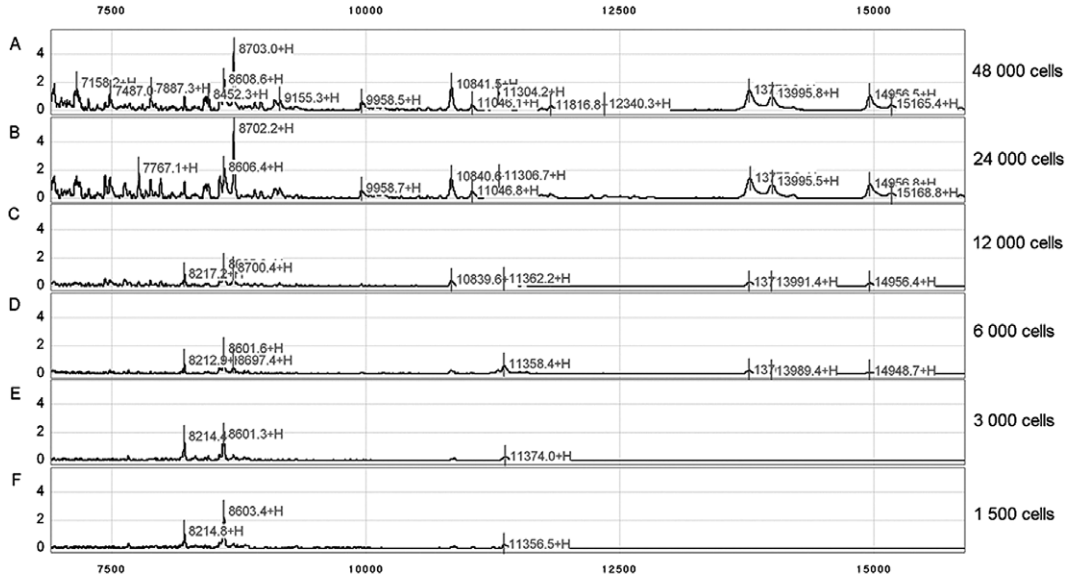

Fig. 2. Determination of the minimal input of B-cells for SELDI-TOF MS based protein profiling. Mass spectra were generated from different numbers of laser dissected germinal centre B-cells: 48,000, 24,000, 12,000, 6,000, 3,000 and 1,500 cells (Fig. 2A–F, respectively). For all spectra generated, the segment from 7,500–15,000 M/Z is shown. Prior to analysis, a lysate of approximately 48,000 laser dissected B-cells was quantified and corresponded to 4 ug of whole protein.

from 48,000 and 24,000 germinal centre cells (Fig. 2). Lower cell numbers showed a major decrease in peak intensities. We therefore decided to use 48,000 cells, where 48,000 B-cells correspond to 4 ug of whole protein. This amount corresponds to approximately 3 mm^2 of a 10 um frozen tissue section and illustrates the small size of this sample.

3.2. *Protein profiling of B-cell non-Hodgkin's lymphoma*

We have analyzed protein lysates from frozen tissue sections of cases of DLBCL ($n = 8$), FL ($n = 8$) and MCL ($n = 8$). The group of benign lymph nodes consisted of different types of RL ($n = 14$). To assess intra-experiment and inter-experiment variation, we have analysed fifteen replicate samples on two different days. Please note that all these thirty spots were each on a different chip. The pooled relative variation (%CVp) values for intra-experimental variation of the ion intensities for day 1 and day 2 were 31.5% and 34.8%, respectively. The inter-experiment %CVp resulting from these experiments is 35.4%. These values are comparable to previous reports [22,23].

In this study, ninety-four clusters were detected using the criteria described in Section 2.6. P-values should be <0.00053 $(0.05/94)$ to be significant (Bonferroni correction for multiple testing). We detected multiple peaks that differentiated between the different lymphoma types. One example is a peak at M/Z 5,567, which significantly differentiates DLBCL from the other lymphoma types and the RL (Kruskal–Wallis H test, p-value $= 0.00002$) (Fig. 3A, D). An additional classifier peak at M/Z $= 2{,}384$ is applicable for further differentiation between benign lymph node cases and the cases of FL and MCL (Kruskal–Wallis H test, p-value $= 0.0002$) (Fig. 3B, E). A third example of a differentially expressed peak is at M/Z $= 15{,}106$ that discriminates between MCL and FL cases, however not significantly (Mann–Whitney U test, p-value $= 0.12$) (Fig. 3C, F).

Although the case numbers are relatively limited, a supervised classification algorithm was constructed based on the differentially expressed peaks detected. The algorithm was internally validated using 8-fold cross validation resulting in the development of the most optimal classification tree. The resulting algorithm (Fig. 4) combines three peaks to classify the lymphoma cases and discriminate them from the benign lesions. The predicted classification success was 75% for follicular lymphoma and 87.5% for diffuse large B-cell lymphoma; for mantle cell lymphoma the predicted success was 37.5% (Table 1A and B).

We also performed unsupervised clustering for the detected peak-clusters (Fig. 5). This approach uses all clusters (peaks) to evaluate which cases are most sim-

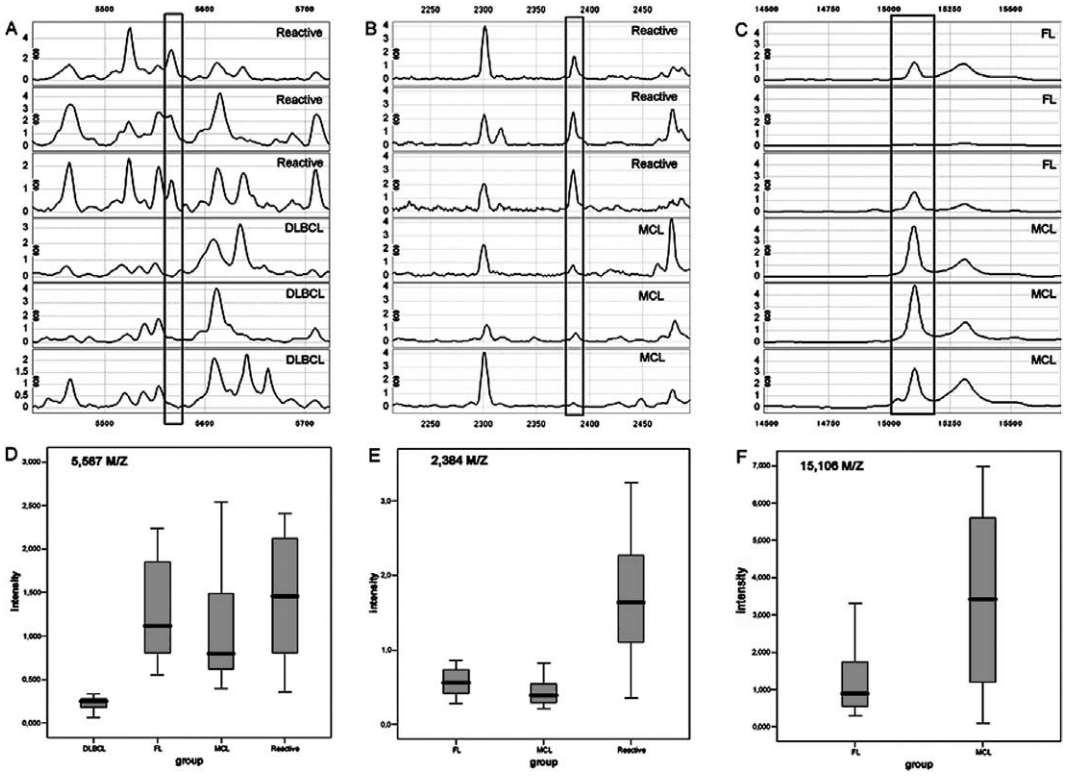

Fig. 3. SELDI-TOF MS enables detection of differentially expressed proteins in lymphoma tissue samples. Examples of three differentially expressed peaks are shown in panels A–C. A small peak at M/Z 5,567 is detected in reactive benign nodes, FL and MCL but is absent in cases of DLBCL (p–value < 0.00002) (Fig. 3A). Similarly, a peak at M/Z 2,384 is expressed in benign reactive nodes, but this peak is almost absent in the spectra of MCL and FL cases (p-value < 0.0002) (Fig. 3B). A third example of a peak at M/Z 15,106 shows a differential expression, however the difference is not significant (p-value $= 0.12$) (Fig. 3C). The lower panels (Fig. 3D–E) show the corresponding box-whisker plots for the mean intensities (Y-axis) of the peaks at M/Z 5,567, 2,384 and 15,106 respectively. The different groups are plotted along the X-axis.

ilar. A large cluster of predominantly RL nodes and FL cases was formed on the right and a cluster of predominantly DLBCL and MCL cases was formed on the left (groups are indicated with coloured lines). However, this clustering is not entirely according the pathological classification. It is important to realise though that there may be many sample characteristics reflected at the protein level and thus in the protein profiles, thereby possibly influencing the unsupervised clustering. This is probably observed for several cases of the FL group that cluster next to the benign cases. These FL cases harbour many T-cells and dendritic cells, as do the benign cases and may explain why they are clustered together. In contrary, DLBCL case 11 and 12 have a relatively low tumour load of 50% and this may account for their clustering separately from the other DLBCL with higher tumour loads (Table 3). Furthermore, MCL and DLBCL are both regarded as intermediate aggressive lymphoma and their joint clustering in two neighbouring branches may be reflecting this clinical behaviour in some way. Unsupervised clustering of the fourteen benign, reactive lymph node cases as a separate group showed no evident clustering based on hyperplasia type (Fig. 6). The composition of these reactive lymph nodes regarding the amount and combination of hyperplasia types was assessed using H&E stained tissue sections adjacent to the sections used for LDM (Table 2). Also, protein profiles generated from laser micro dissected hyperplasia types showed many similarities (Fig. 7).

4. Discussion

In this study we have optimized a protocol for SELDI-TOF MS based protein profiling of small lymphoma tissue samples that allowed detection of many unique peaks. With the set criteria (Section 2.6), ninety-four unique peaks were detected of which many were differentially expressed.

Table 1

Classification results for the supervised classification algorithm. The actual classification results for the generated supervised algorithm are shown (Table 1A) together with the predicted classification results (Table 1B), obtained after V-fold cross validation

			Predicted class			
Actual class	Total cases	Percent correct	DLBCL $n = 8$	FL $n = 8$	MCL $n = 8$	Benign $n = 8$
DLBCL	8	100	8	0	0	0
FL	8	100	0	8	0	0
MCL	8	75	0	2	6	0
Benign	14	86	0	2	0	12

A: actual classification result.

			Predicted class			
Actual class	Total cases	Percent correct	DLBCL $n = 8$	FL $n = 8$	MCL $n = 8$	Benign $n = 8$
DLBCL	8	87.5	7	0	0	1
FL	8	75.0	0	6	2	0
MCL	8	37.5	0	5	3	0
Benign	14	85.7	0	2	0	12

B: predicted classification after V-fold cross-validation.

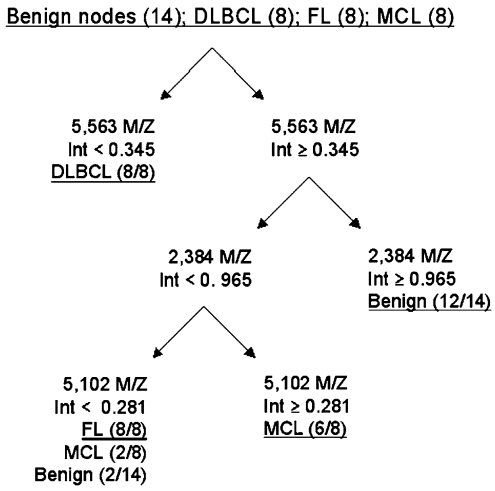

Fig. 4. SELDI-TOF MS based supervised classification algorithm for the classification of DLBCL, FL, MCL and benign lymph nodes. The algorithm is illustrated as a decision-tree with three splits or classifier peaks. The classifier peaks are given by their M/Z values in combination with the intensity (int) threshold used for classification. The underlined sample group is the one that predominates the resulting group after classification; the number of cases present of each group is indicated between brackets.

Using laser dissection microscopy, we have determined that only very small parts of frozen tissue biopsies, corresponding to about 3 mm^2 of 10 μm frozen tissue section or approximately 50,000 cells, are already sufficient to generate SELDI-TOF mass spectra. The dissected samples were independently collected and are therefore not identical, resulting in some very subtle differences between the spectra of 24,000 and 48,000 cells. Cell numbers ranging between 500–5,000 cells per sample have been reported in SELDI-TOF MS studies before [15,24]. However, these studies used epithelial cells that are much larger and contain more proteins than the B- and T-cells from the lymphoma specimens used in this study. The small size of the tissue sections required for analysis allows the use of this technique when limited diagnostic material is available in case of, for example, core needle biopsies or fine needle aspirates of tissues suspect for lymphoma.

With our specific protocol for tissue samples we showed that differentially expressed peaks between benign nodes, DLBCL and small B-cell lymphoma subtypes (including FL and MCL) were detected by SELDI-TOF MS. These differentially expressed peaks have been used for the generation of a supervised classification algorithm. Because supervised classification is prone to over fitting we applied internal V-fold cross validation for the generation of the algorithm. The resulting estimations of classification errors give insight into the predicted classification success of the algorithm. With our specific protocol for tissue samples we showed that DLBCL can be reliably identified. Univariate differentiation of MCL and FL was not significant in this study. The unsupervised

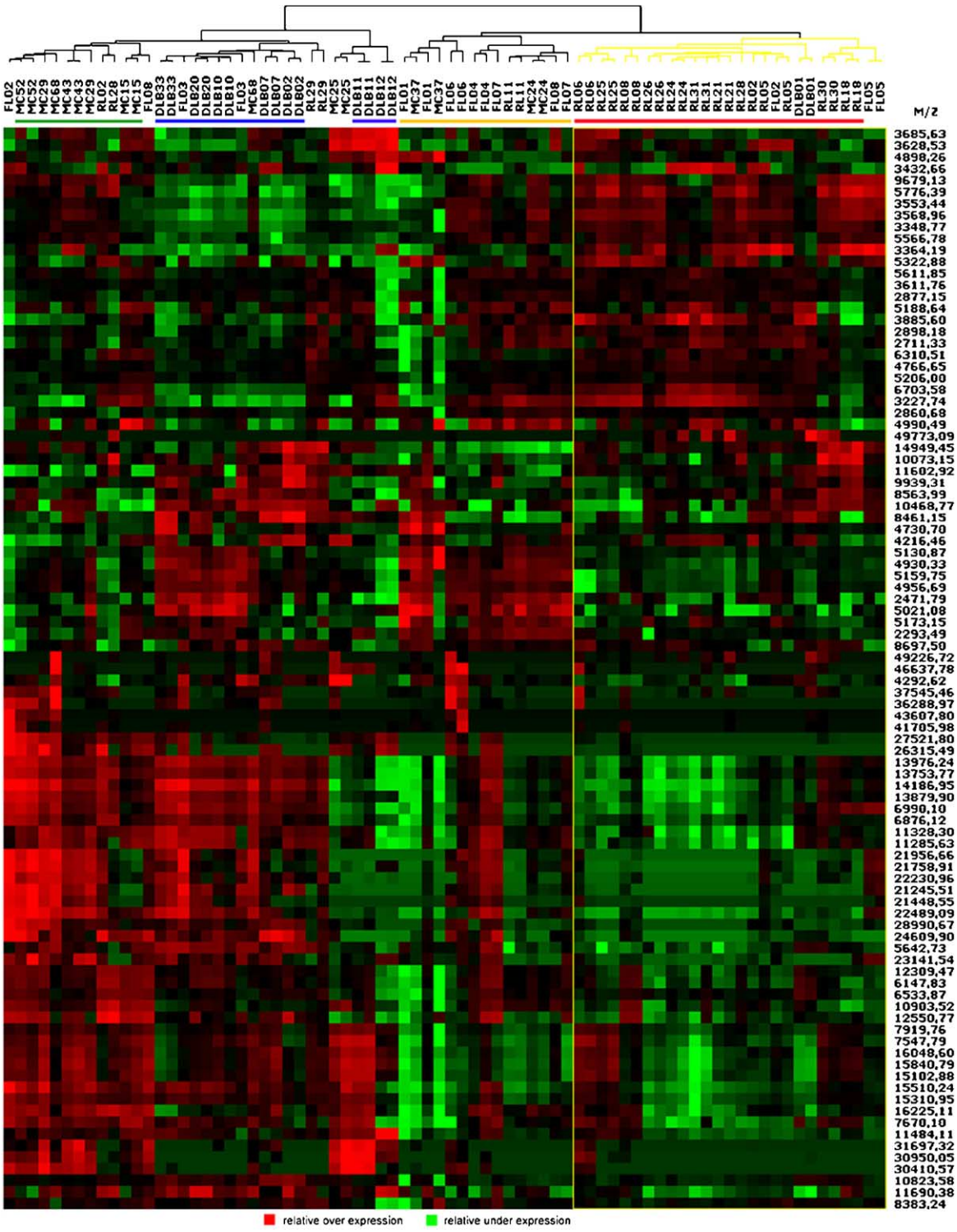

Fig. 5. Unsupervised clustering of SELDI-TOF MS data of reactive lymph nodes, DLBCL, FL and MCL. Along the X-axis are the lymphoma cases (each case in duplicate) (MC = MCL; DLB = DLBCL; RL = benign lymph node) and along the Y-axis are the M/Z values of the peaks that were generated in these spectra and these peaks are all used in this unsupervised clustering. On the right, a cluster of benign, reactive lymph nodes (red bar) and FL cases (yellow bar) is formed, and on the left DLBCL (blue bar) and MCL (green bar) cases cluster together.

Table 2

Hyperplasia composition of RL cases in the classification study. Case replicates are listed in the table according to their order in the unsupervised clustering with the first case in the list corresponding to the most left one in the image (Fig. 6). The hyperplasia composition was assessed on the adjacent H&E stained sections, and was expressed as the relative area of the whole section

Cluster order	Sample name	Hyperplasia type (% area)		
		% area B-cell	% area T-cell	% area sinus
1	RL11	40	50	10
2	RL11	40	50	10
3	RL08	50	45	5
4	RL08	50	45	5
5	RL24	75	15	10
6	RL31	70	25	5
7	RL24	75	15	10
8	RL31	70	25	5
9	RL02	45	10	45
10	RL05	0	95	5
11	RL05	0	95	5
12	RL21	80	10	10
13	RL21	80	10	10
14	RL26	15	75	10
15	RL25	0	90	10
16	RL25	0	90	10
17	RL28	0	50	50
18	RL26	15	75	10
19	RL06	80	15	5
20	RL06	80	15	5
21	RL02	45	10	45
22	RL28	0	50	50
23	RL29	20	75	5
24	RL29	20	75	5
25	RL30	40	50	10
26	RL30	40	50	10
27	RL18	70	20	10
28	RL18	70	20	10

clustering showed apparent grouping according to, on the right hand side, a benign/indolent profile and, on the left hand side, a more aggressive clinical behaviour. This also suggests that the generated protein profiles contain potentially clinically relevant information. Identification of discriminating proteins from both the unsupervised and the supervised analysis is an important next step, not only to provide insight into the nature of these proteins, but also for subsequent validation, and possible application of classifier proteins as new biomarkers in immunohistochemistry or cytochemistry. As shown in Fig. 6, hyperplasia type does not direct the unsupervised clustering of this heterogeneous group of benign, reactive lymph nodes. Apparently, other factors than merely phenotype related ones, drive their clustering. This is an important observation because this implies that protein profiling based classification of benign and malignant lymph nodes would not be complicated by this heterogeneity.

Table 3

Tumour load of NHL cases in the proteomics study. The tumour load was assessed using adjacent H&E stained sections, and was expressed as the relative area of the whole section

Sample	Tumour load (% area)	Grade
FL01	60	IIIa
FL02	85	I
FL03	60	IIIa
FL04	75	IIIa
FL05	50	I
FL06	70	IIIa
FL07	60	IIIa
FL08	80	IIIa
MC15	75	
MC24	65	
MC25	>90	
MC29	90	
MC37	90	
MC43	90	
MC52	90	
MC68	>90	
DLB01	80	
DLB02	80	
DLB07	90	
DLB10	90	
DLB11	50	
DLB12	50	
DLB20	90	
DLB33	90	

Samples in our study were obtained from whole tissue sections without dissection of tumour cells, despite the fact that lymph nodes and lymphomas are heterogeneous in cell and stroma composition. The relevance of stroma and micro-environment for tumour biology and classification is increasingly recognized [25,26]. Because of this, we have intentionally included the micro-environment of the tumour, in contrast to earlier tissue profiling studies that have selected tumour cells by LDM prior to protein profiling [27, 28]. The studied subcategories of B-NHL each have

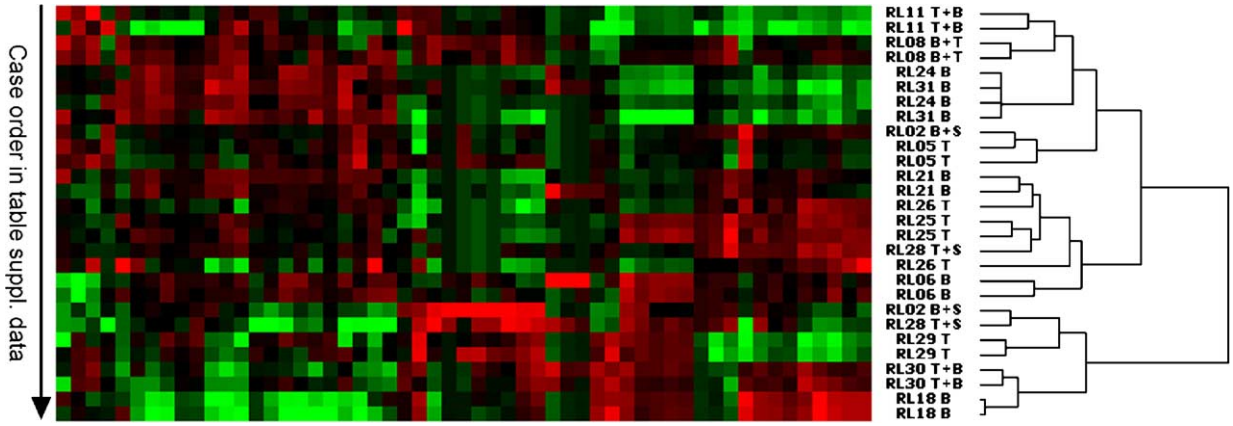

Fig. 6. Unsupervised classification of the reactive lymph node cases that contain different combinations and amounts of B-cells, T-cells and sinus histiocytosis. Along the Y-axis are the benign lymph node cases (each case in duplicate) (RL = benign lymph node). Behind the sample name is indicated which hyperplasia type and thus which cell type is predominantly present in the sample (B: B-cells or follicular hyperplasia, T: T-cells or paracortical hyperplasia, and S: sinus histiocytosis). Detailed information on hyperplasia composition is provided in Table 2.

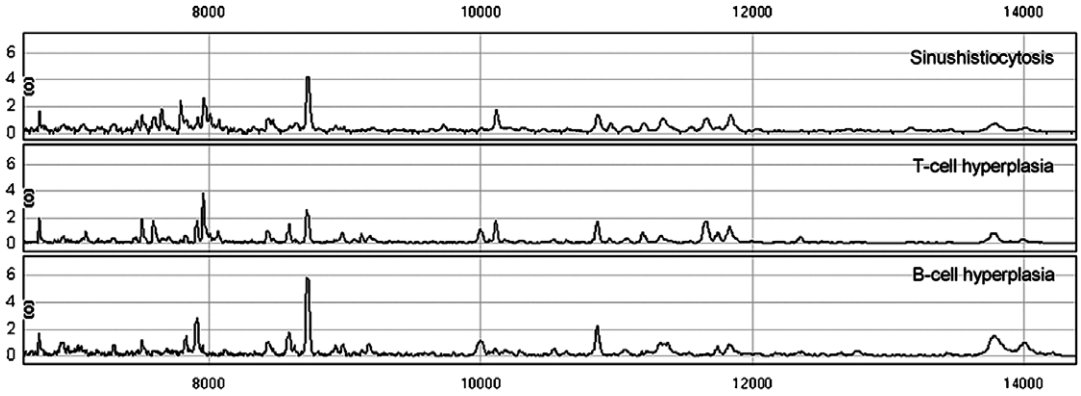

Fig. 7. Comparison of protein profiles from three benign hyperplasia types. Protein profiles were generated from laser micro dissected cells from reactive hyperplasia types often seen in benign lymph nodes: sinus histiocytosis (upper spectrum), paracortical hyperplasia (predominantly T-cells) (middle spectrum), and follicular hyperplasia (mainly B-cells) (lower spectrum). The segment from 7,000–14,000 M/Z is shown here (Y-axis).

a unique micro-environment. For example, FL has a cellular micro-environment of T-helper cells and dendritic cells, while DLBCL and MCL can harbour many macrophages. These factors, as well as tumour load are expected to determine the concentration and the relative peak intensity for individual classifier peaks and might influence the supervised classification results, since intensity thresholds are set for each of the classifier peaks used. Important to realize is that classifier peaks may derive from both the tumour cells as well as the stroma or micro-environment, as demonstrated by a specific protein biomarker for pancreatic duct carcinoma that most likely is derived from the benign adjacent acini and not from the carcinoma itself [29].

5. In conclusion

Our study shows that SELDI-TOF MS based protein profiling of small histological samples without dissection of tumour cells is feasible. Moreover, differentiation of NHL types and benign lymph nodes through the generation of a internally validated classification algorithm using differentially expressed peaks was feasible although larger studies are required for improved classification results. The identified classifiers may provide potentially new biomarkers for use in immunohisto- or cytochemistry. This method is applicable to many other samples and therefore represents a potential tool in clinical pathology, especially when only limited tissue is available.

Acknowledgements

The authors thank Arnoud Loof for his support with the SELDI-TOF MS experiments and Henry Dijkman for his advice in the laser dissection microscopy.

Leica Microsystems Wetzlar GmbH (D) is acknowledged for their financial support of the laser dissection microscopy experiments. Leica Microsystems Wetzlar GmbH (D) had no involvement in the study design, in the collection, analysis and interpretation of data, in writing the report or in the decision to submit the report for publication.

References

[1] E.S. Jaffee, N.L. Harris, H. Skin and J.W. Vardiman (eds), *World Health Organization Classification of Tumors. Pathology and Genetics of Tumors of Hematopoietic and Lymphoid Tissues*, IARC Press, Lyon, 2001.

[2] M.S. Lim and K.S. Elenitoba-Johnson, Mass spectrometry-based proteomic studies of human anaplastic large cell lymphoma, *Mol. Cell. Proteomics* **5**(10) (2006), 1787–1798.

[3] K.S. Elenitoba-Johnson, D.K. Crockett, J.A. Schumacher, S.D. Jenson, C.M. Coffin, A.L. Rockwood et al., Proteomic identification of oncogenic chromosomal translocation partners encoding chimeric anaplastic lymphoma kinase fusion proteins, *Proc. Natl. Acad. Sci. USA* **103**(19) (2006), 7402–7407.

[4] C.P. Vaughn, D.K. Crockett, Z. Lin, M.S. Lim, K.S. Elenitoba-Johnson, Identification of proteins released by follicular lymphoma-derived cells using a mass spectrometry-based approach, *Proteomics* **6**(10) (2006), 3223–3230.

[5] M.P. Ebert, J. Meuer, J.C. Wiemer, H.U. Schulz, M.A. Reymond, U. Traugott et al., Identification of gastric cancer patients by serum protein profiling, *J. Proteome Res.* **3**(6) (2004), 1261–1266.

[6] E.T. Fung, T.T. Yip, L. Lomas, Z. Wang, C. Yip, X.Y. Meng et al., Classification of cancer types by measuring variants of host response proteins using SELDI serum assays, *Int. J. Cancer* **115**(5) (2005), 783–789.

[7] J. Koopmann, Z. Zhang, N. White, J. Rosenzweig, N. Fedarko, S. Jagannath et al., Serum diagnosis of pancreatic adenocarcinoma using surface-enhanced laser desorption and ionization mass spectrometry, *Clin. Cancer Res.* **10**(3) (2004), 860–868.

[8] J. Li, Z. Zhang, J. Rosenzweig, Y.Y. Wang and D.W. Chan, Proteomics and bioinformatics approaches for identification of serum biomarkers to detect breast cancer, *Clin. Chem.* **48**(8) (2002), 1296–1304.

[9] V. Paradis, F. Degos, D. Dargere, N. Pham, J. Belghiti, C. Degott et al., Identification of a new marker of hepatocellular carcinoma by serum protein profiling of patients with chronic liver diseases, *Hepatology* **41**(1) (2005), 40–47.

[10] S.Y. Yang, X.Y. Xiao, W.G. Zhang, L.J. Zhang, W. Zhang, B. Zhou et al., Application of serum SELDI proteomic patterns in diagnosis of lung cancer, *BMC Cancer* **5** (2005), 83–90.

[11] Y. Yu, S. Chen, L.S. Wang, W.L. Chen, W.J. Guo, H. Yan et al., Prediction of pancreatic cancer by serum biomarkers using surface-enhanced laser desorption/ionization-based decision tree classification, *Oncology* **68**(1) (2005), 79–86.

[12] T. Yoshizaki, T. Enomoto, R. Nakashima, Y. Ueda, H. Kanao, K. Yoshino et al., Altered protein expression in endometrial carcinogenesis, *Cancer Lett.* **226**(2) (2005), 101–106.

[13] T.A. Zhukov, R.A. Johanson, A.B. Cantor, R.A. Clark, M.S. Tockman, Discovery of distinct protein profiles specific for lung tumors and pre-malignant lung lesions by SELDI mass spectrometry, *Lung Cancer* **40**(3) (2003), 267–279.

[14] Y.F. Wong, T.H. Cheung, K.W. Lo, V.W. Wang, C.S. Chan, T.B. Ng et al., Protein profiling of cervical cancer by protein-biochips: proteomic scoring to discriminate cervical cancer from normal cervix, *Cancer Lett.* **211**(2) (2004), 227–234.

[15] G. Kwapiszewska, M. Meyer, R. Bogumil, R.M. Bohle, W. Seeger, N. Weissmann et al., Identification of proteins in laser-microdissected small cell numbers by SELDI-TOF and Tandem MS, *BMC Biotechnol.* **4** (2004), 30–40.

[16] I.N. Lee, C.H. Chen, J.C. Sheu, H.S. Lee, G.T. Huang, D.S. Chen et al., Identification of complement C3a as a candidate biomarker in human chronic hepatitis C and HCV-related hepatocellular carcinoma using a proteomics approach, *Proteomics* **6**(9) (2006), 2865–2873.

[17] G. Malik, M.D. Ward, S.K. Gupta, M.W. Trosset, W.E. Grizzle, B.L. Adam et al., Serum levels of an isoform of apolipoprotein A-II as a potential marker for prostate cancer, *Clin. Cancer Res.* **11**(3) (2005), 1073–1085.

[18] C. Melle, G. Ernst, B. Schimmel, A. Bleul, H. Mothes, R. Kaufmann et al., Different expression of calgizzarin (S100A11) in normal colonic epithelium, adenoma and colorectal carcinoma, *Int. J. Oncol.* **28**(1) (2006), 195–200.

[19] G. Fan, M. Molstad, R.M. Braziel, M. Standley, J. Huang, W. Rodgers et al., Proteomic profiling of mature CD10+ B-cell lymphomas, *Am. J. Clin. Pathol.* **124**(6) (2005), 920–929.

[20] Z. Lin, S.D. Jenson, M.S. Lim, K.S. Elenitoba-Johnson, Application of SELDI-TOF mass spectrometry for the identification of differentially expressed proteins in transformed follicular lymphoma, *Mod. Pathol.* **17**(6) (2004), 670–678.

[21] Federation of medical Scientific Societies. Code for proper secondary use of human tissue in the Netherlands, http://www.federa.org/?s=1&m=78&p=&v=4, 2002. Ref Type: Internet Communication.

[22] M. Aivado, D. Spentzos, G. Alterovitz, H.H. Otu, F. Grall, A.A. Giagounidis et al., Optimization and evaluation of surface-enhanced laser desorption/ionization time-of-flight mass spectrometry (SELDI-TOF MS) with reversed-phase protein arrays for protein profiling, *Clin. Chem. Lab. Med.* **43**(2) (2005), 133–140.

[23] J. Albrethsen, R. Bogebo, J. Olsen, H. Raskov and S. Gammeltoft, Preanalytical and analytical variation of surface-enhanced laser desorption-ionization time-of-flight mass spectrometry of human serum, *Clin. Chem. Lab. Med.* **44**(10) (2006), 1243–1252.

[24] C. Melle, G. Ernst, B. Schimmel, A. Bleul, S. Koscielny, A. Wiesner et al., Biomarker discovery and identification in laser microdissected head and neck squamous cell carcinoma with ProteinChip(R) technology, two-dimensional gel electrophoresis, tandem mass spectrometry, and immunohistochemistry, *Mol. Cell. Proteomics* **2**(7) (2003), 443–452.

[25] L. Kopfstein and G. Christofori, Metastasis: cell-autonomous mechanisms versus contributions by the tumor microenvironment, *Cell. Mol. Life Sci.* **63**(4) (2006), 449–468.

[26] P. Schedin and A. Elias, Multistep tumorigenesis and the microenvironment, *Breast Cancer Res.* **6**(2) (2004), 93–101.

[27] F. Von Eggeling, H. Davies, L. Lomas, W. Fiedler, K. Junker, U. Claussen et al., Tissue-specific microdissection coupled with ProteinChip array technologies: applications in cancer research, *Biotechniques* **29**(5) (2000), 1066–1070.

[28] C.P. Paweletz, L.A. Liotta and E.F. Petricoin III, New technologies for biomarker analysis of prostate cancer progression: Laser capture microdissection and tissue proteomics, *Urology* **57**(4, Suppl. 1) (2001), 160–163.

[29] C. Rosty, L. Christa, S. Kuzdzal, W.M. Baldwin, M.L. Zahurak, F. Carnot et al., Identification of hepatocarcinoma-intestine-pancreas/pancreatitis-associated protein I as a biomarker for pancreatic ductal adenocarcinoma by protein biochip technology, *Cancer Res.* **62**(6) (2002), 1868–1875.